Uludağ University Journal of The Faculty of Engineering, Vol. 29, No. 1, 2024 RESEARCH

DOI: 10.17482/uumfd.1275351

THE EFFECT OF DIFFERENT DIELECTRIC MATERIALS ON RADIATION FEATURES OF SLOTTED PATCH ANTENNAS FOR 6G COMMUNICATION SYSTEMS

Barış Gürcan HAKANOĞLU *

Received: 02.04.2023; revised: 18.01.2024; accepted: 18.03.2024

Abstract: In this study, patch antenna structures with rhombic shaped slots have been investigated for 6G communication systems. Four different dielectric materials, such as arlon, polyamide, polyimide, and silicon, have been selected for antennas with the same design procedure. In this way, the effects of slots on frequency responses for different dielectric substrates have been searched. The slots are parametrically analyzed in terms of edge size and location, and the designs are completed for values with the lowest return loss levels. The amount of return loss reduction in slotted antennas is 38% and 42% for arlon and polyamide, respectively, while the reduction is 28% and 8% for polyimide and silicon, respectively. In addition, bandwidth increases in slotted antennas vary according to the dielectric substrate material. The bandwidth increases have been 0.05 GHz, 0.426 GHz, 0.839 GHz, and 0.475 GHz for arlon, polyamide, polyimide, and silicon substrates, respectively. With these results, the study will give an insight to the researchers who will design antennas in 6G bands in terms of the effects of materials on antenna characteristics and will give inspiration for new designs.

Keywords: 6G, materials for 6G, patch antennas, THz communication, wireless communication

6G Haberleşme Sistemleri İçin Yarıklı Yama Antenlerde Farklı Dielektrik Malzemelerin Yayılma Karakteristiklerine Etkisi

Öz: Bu çalışmada 6G haberleşme sistemleri için eşkenar dörtgen şekilli yarıklara sahip yama anten yapıları incelenmiştir. Aynı tasarım prosedürüne sahip antenlerde arlon, polyamit, polyimit ve silikon olmak üzere dört farklı dielektrik malzeme kullanılmıştır. Bu şekilde yarık etkilerinin farklı dielektrik tabanlarda frekans cevaplarına etkileri araştırılmıştır. Yarıklar, kenar boyutu ve konum olarak parametrik analizlere tabi tutulmuşlardır ve tasarımlar en az geri dönüş kaybına sahip değerler için tamamlanmıştır. Yarıklı antenlerde geri dönüş kaybı azalma miktarı arlon ve polyamit için sırasıyla %38 ve %42 olurken, polyimit ve silikon için sırasıyla %28 ve %8 olmuştur. Ek olarak yarıklı antenlerde bant genişliği kazançları dielektrik taban malzemesine göre değişkenlik göstermiş, bant genişliği artışları arlon, polyamit, polyimit ve silikon tabanlar için sırasıyla 0,050 GHz, 0,426 GHz, 0,839 GHz ve 0,475 GHz olmuştur. Bu sonuçlarla çalışma, 6G bantlarında anten tasarımı yapacak araştırmacılara malzemelerin anten karakteristikleri üzerindeki etkileri açısından fikir verecek ve yeni tasarımlar için ilham kaynağı olacaktır.

Anahtar Kelimeler: 6G, 6G için malzemeler, yama antenler, THz haberleşme, kablosuz haberleşme

* Bandırma Onyedi Eylül University Faculty of Engineering and Natural Sciences, Electrical-Electronics Eng. Dept. Central Campus 10200 Bandırma/Balıkesir
Corresponding Author: Barış Gürcan Hakanoğlu (bhakanoglu@bandirma.edu.tr)
This article is an extended version of the conference paper entitled by "6G Haberleşme Sistemleri İçin Yarıklı Yama Antenlerde Farklı Dielektrik Malzemelerin Yayılma Karakteristiklerine Etkisi" and presented orally at the ELECO'2022 Symposium, which was invited by the symposium executive board to be evaluated in the Uludağ University Journal of the Faculty of Engineering.

1. INTRODUCTION

The increase in applications that use large amounts of data in wireless communication systems encourages researchers to develop technologies that can enable faster transmission. As the fifth generation (5G) communication systems enter our lives, researches have already started to meet the needs in the 2030s and it is expected that the next communication systems will be used as the sixth generation (6G) in these years. Especially with the use of the terahertz (THz) band (Giordani et al., 2020; Yang et al., 2019), it will be necessary to provide high time and phase simultaneity beyond the needs of 5G systems (You et al., 2021). With the full integration of artificial intelligence into the 6G communication system, developments such as augmented reality, interconnected robotic and autonomous systems, smart health and biomedical communication systems, internet of everything and even data transfer of the five senses will be a part of our daily lives (Chowdhury et al., 2020; Alsharif et al., 2020). In addition, these new developments will contribute to the studies to be carried out for the adaptation of communication systems to the THz band (Strinati et al., 2022).

As in previous generations, antennas will be the important focus for 6G communication. Similar to the microwave and millimeter wave spectrum, patch antennas are among the most researched antenna types for 6G systems with their low cost, ease of analysis and advantageous radiation characteristics. A new high-gain patch antenna array structure has been proposed for autonomous vehicles in 6G wireless systems and a gain of 18 dB has been obtained (Foysal et al., 2021). A patch antenna design for partial discharge detection for device monitoring systems in smart networks is designed for ultra-wideband (UWB) operation based on 6G-IoT (Internet of Things) (Ilahi et al., 2021). Additionally, the behavior of different dielectric materials in THz region for UWB antennas is investigated for an elliptical patch antenna and has been found that the impedance bandwidth is increased up to 5 THz with the partial design of the ground plane (Singhal et al., 2019). A patch antenna operating in the 279 GHz-305 GHz band is designed using silicon-based technology and 0.18 μm CMOS (Complementary Metal Oxide Semiconductor) method and proposed for 6G communication applications (Chung et al., 2021). In addition, graphene has attracted much attention with its advantageous conductivity properties and has been extensively researched in patch antenna designs. A square-shaped graphene patch antenna design on a silicon dioxide dielectric substrate is designed for the 12.2-13.8 THz band, and the analysis results for different parameters of the antenna have been investigated (Bala et al., 2016). The properties of a conventional patch antenna using copper as a conductor in the 0.7 THz region were compared with the results obtained using a graphene patch for the same frequency, and it was found that the use of graphene provided more gain and lower return loss for this frequency (Azizi et al., 2017). Another study about a graphene nano-stripe-based patch antenna was designed for the 725-775 GHz band on a 20 μm thick polyimide substrate and a radiation efficiency of 86.58% was achieved (Anand et al., 2014). A bandwidth of 504 GHz has been obtained with the graphene circular patch antenna designed on the silicon substrate proposed for device-to-device communication in the THz band (Dashti et al., 2018). In addition, the effect of dielectric substrates with different geometric shapes on the operating frequencies of graphene patch antennas has been investigated (Khan et al., 2020), performance increases have been achieved with metasurfaces in graphene antennas (Efazat et al., 2019), and dual-band operation has been provided for graphene-based miniaturized antennas (Khan et al., 2019).

In this study, patch antennas operating in the THz band have been designed with different dielectric substrates such as arlon, polyamide, polyimide and silicon. Rhombic shaped slots have been etched on the patch. These slots have been designed by following the same design procedure on each antenna structure and performed many parametric analyzes in terms of both edge dimensions and positions. In this way, frequency responses for each antenna have been obtained for different materials. The proposed work will be helpful in understanding the antenna

characteristics for different dielectric materials of the designs to be executed in microsterip patch antennas at 6G frequencies.

2. DESIGN

Antennas propsed for 6G communication systems are designed in computer environment with Computer Simulation Technology Microwave Studio (CST MWS) software (CST, 2016). The dielectric materials used for the antennas have been selected as arlon, polyamide, polyimide, and silicon. The dielectric constants are 3.43, 4.3, 3.5, 11.9 for arlon, polyamide, polyimide, and silicon, respectively. In the selection of these materials, the studies in the literature have been taken into account (Singhal et al., 2019; Chung et al., 2021; Bala et al., 2016; Azizi et al., 2017). The heights of the dielectric substrates have been taken as 6 μm for arlon, polyamide and polyimide, and 6.5 μm for silicon. These heights have been chosen in such a way that $h<<\lambda_0$ condition is met (Balanis, 2005). Here λ_0 denotes the empty space wavelength. In addition, the copper thickness, t, is adjusted for $t<<\lambda_0$, which is also a design condition for microstrip patch antennas and should be met (Balanis, 2005).

2.1. Design Equations

Reference antennas are designed according to the rectangular microstrip patch antenna transmission line equivalent (Stutzmann, 1998). Equations 1-4 show the calculations to be performed according to this equivalent. In these expressions, f represents the operating frequency and c represents the speed of light. The width and the length of the patch are shown by W_{patch} and L_{patch}, respectively. The material parameters such as the dielectric constant and the height of the substrate are depicted by ε_r and h, respectively. After determining the operating frequency, the height and dielectric constant of the substrate, the width of the antenna has been calculated according to Equation 1. Then, the elongation due to scattering has been considered with Equation 2 and Equation 3, and finally, the length of the antenna has been calculated with Equation 4.

$$W_{patch} = \frac{c}{2f_r}\sqrt{\frac{2}{\varepsilon_r + 1}} \tag{1}$$

$$\varepsilon_{eff} = \frac{\varepsilon_r + 1}{2} + \frac{\varepsilon_r - 1}{2}\left[1 + 12\frac{h}{W_{patch}}\right]^{-\frac{1}{2}} \tag{2}$$

$$\frac{\Delta L_{patch}}{h} = 0.412\frac{\left(\varepsilon_{eff} + 0.3\right)\left(\frac{W_{patch}}{h} + 0.264\right)}{\left(\varepsilon_{eff} - 0.258\right)\left(\frac{W_{patch}}{h} + 0.8\right)} \tag{3}$$

$$L_{patch} = \frac{c}{2f_r\sqrt{\varepsilon_{eff}}} - 2\Delta L_{patch} \tag{4}$$

Then according to the design procedure of square patch antenna the width and the length dimensions are taken equal (Stutzmann, 1998). Equation 5 shows this step.

$$W_{patch} = L_{patch} = \frac{c}{2f_r\sqrt{\frac{\varepsilon_r + 1}{2}}} \tag{5}$$

2.2. New Antenna Structures

Figure 1 represents the general structure and parameter definitions of the antennas designed according to the design procedure. In the figure, the parameters in the x-axis direction are the width of the antenna and the parameters in the y-axis direction are the parameters used for the antenna's length. The design procedure with each different dielectric is the same. Microstrip line and inset feeding method have been used as feeding method. Here, L_{feed} denotes the length of the microstrip line, W_{feed} denotes the width of the microstrip line, F_i is the length of the inset feeding line, and g is the width of the inset feeding line. These parameters are optimized for antenna input impedance of 50 ohms.

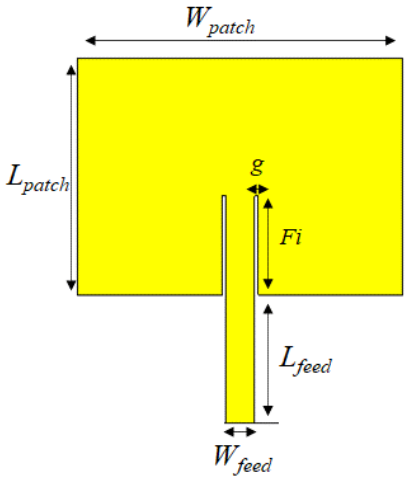

Figure 1:
Patch antenna design parameters

The design processes have been repeated for antennas designed with other dielectric materials to operate at 1 THz, and reference antennas are created. Figure 2a-d shows the final model of each reference antenna. The design parameters for each antenna are shown in Table 1-4.

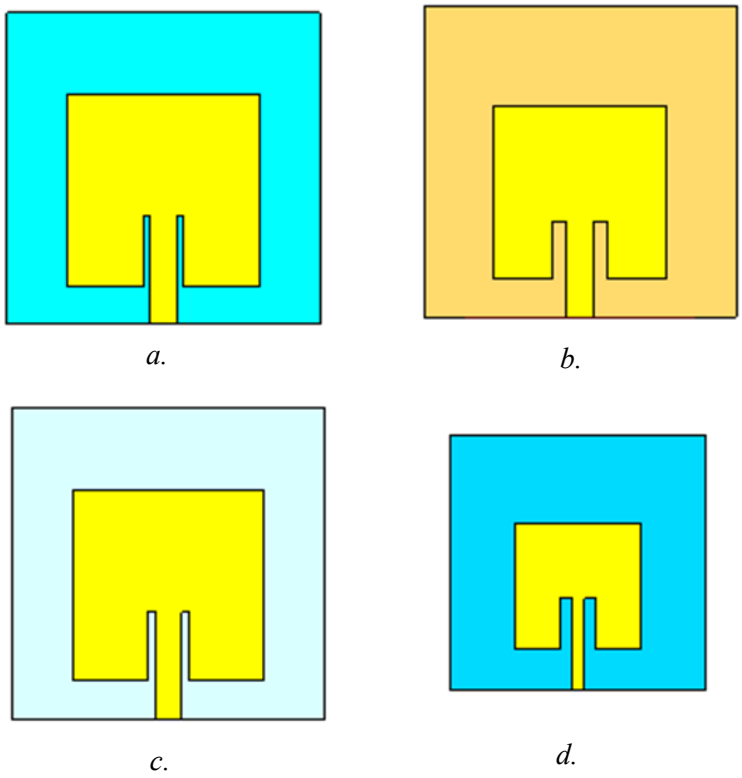

Figure 2:
Reference antennas for four different dielectric material;
a. *Arlon* ***b.*** *Polyamide* ***c.*** *Polyimide* ***d.*** *Silicon*

Table 1. Design parameter values for Arlon (µm)

W_{patch}	L_{patch}	W_{subs}	L_{subs}	g
79.7	79.7	130	130	2.7
F_i	W_{feed}	L_{feed}	t	h
29	11	16	1	6

Table 2. Design parameter values for Polyamide (µm)

W_{patch}	L_{patch}	W_{subs}	L_{subs}	g
72	72	130	130	6
F_i	W_{feed}	L_{feed}	t	h
24	11	16	1	6

Table 3. Design parameter values for Polyimide (µm)

W_{patch}	L_{patch}	W_{subs}	L_{subs}	g
79.7	79.7	130	130	2.86
F_i	W_{feed}	L_{feed}	t	h
29	11	16	1	6

Table 4. Design parameter values for Silicon (µm)

W_{patch}	L_{patch}	W_{subs}	L_{subs}	g
42.5	42.5	86	86	4
F_i	W_{feed}	L_{feed}	t	h
17	4	14	1	6.5

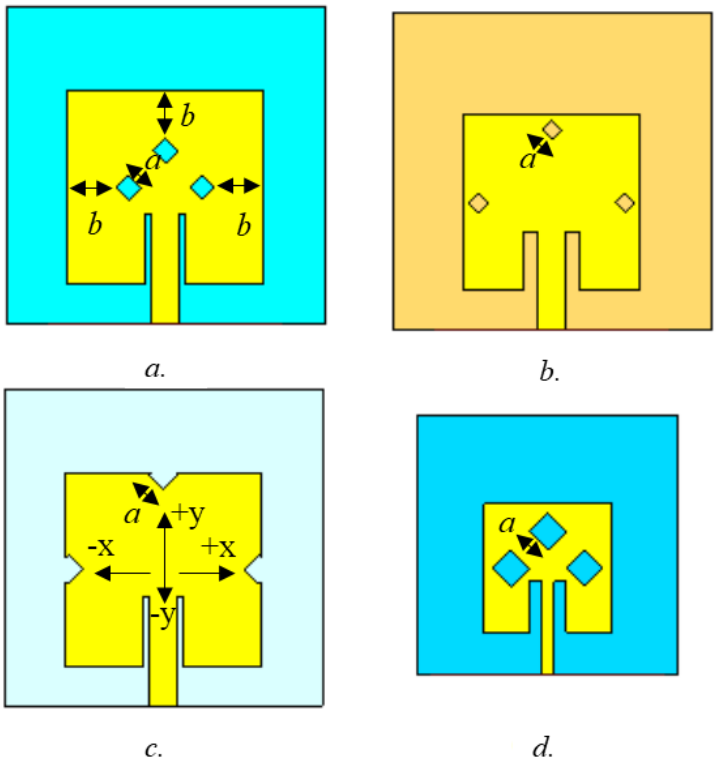

Figure 3:
Proposed antenna models for each dielectric material;
a. *Arlon* ***b.*** *Polyamide* ***c.*** *Polyimide* ***d.*** *Silicon*

In the proposed antenna model, three rhombic shaped slots have been etched on the radiating part. These slots have been first designed in such a way that one of their corners is in the midpoint of

the two side edges and the upper edge of the antenna. Then, while performing the parametric analyses the slots close to the side edges have been shifted in ±x direction denoted by the parameter of *b*, and the slot close to the upper edge has been shifted in ±y direction denoted by the same parameter of *b* becuase the shifting amounts from the edges are all the same. Additionally, the slot edge dimension is denoted by the parameter of *a*. The design is terminated in the position with the lowest level of return loss of the antenna. Due to the different responses of dielectric materials for the same frequency, the final value of the slot edge size and location in each material is different. For example, for polyimide, the slots protrude from the edges, while for arlon, polyamide and silicon the slots remain at the patch boundaries. The final version of the design for each material is shown in Figure 3a-d.

3. RESULTS

Parametric analyzes of the reference antennas and the proposed antennas have been performed and the graphs of the values with the lowest return loss level have been plotted according to the frequency. Figure 4a-b and Figure 5a-b show the comparative frequency responses of the reference antenna and slotted antennas designed with arlon, polyamide, polyimide and silicon dielectric materials, respectively, in the 0.4-1.6 THz range.

3.1. Frequency Responses for the Proposed Models

In the graphics, Antenna1 represents the reference antenna and Antenna 2 represents the slotted antenna model. Looking at the results, it is seen that rhombic shaped slots have a greater effect on antenna return losses for arlon and polyamide substrates than on the return losses for polyimide and silicon substrates.

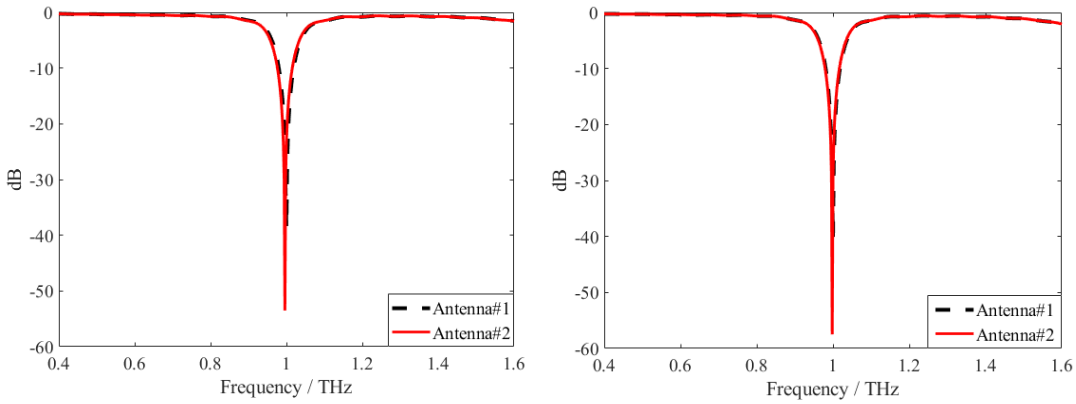

Figure 4:
Return loss plots of reference and slotted antennas;
a. *with arlon substrate* ***b.*** *with polyamide substrate*

While the reference antenna return loss level for the arlon substrate is -38.68 dB, this level decreases to -53.51 dB with the proposed model. In addition, for the polyamide material, the return loss level, which was -40.47 dB in the reference antenna, decreases to -57.48 dB. On the other hand, the return loss level decreases from -35.61 dB to -45.48 dB for polyimide, and from -38.09 dB to -41.17 dB for silicon substrate. Additionally, looking at the bandwidth changes, it is noted that the 10 dB bandwidths span from 39.085 GHz to 39.135 GHz for arlon, from 37.702

GHz to 38.128 GHz for polyamide, from 38.522 GHz to 39.361 GHz for polyimide, and from 44.511 GHz to 44.986 GHz for silicon.

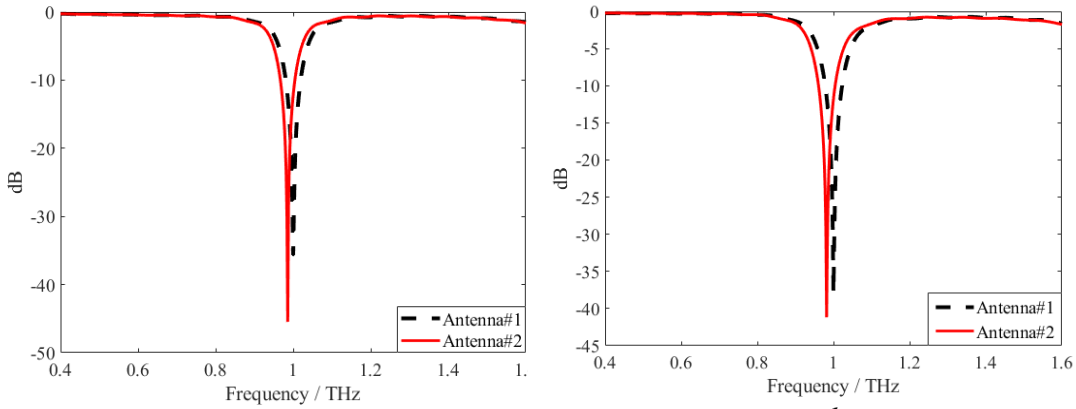

Figure 5:
Return loss plots of reference and slotted antennas;
a. *with polyimide substrate* ***b.*** *with silicon substrate*

If we evaluate the frequency shifts for the four materials, the frequency shifts for the polyamide and silicon substrates are greater than the shifts for the arlon and polyamide substrates. In general, when slots are loaded to the microstrip patch antenna, it corresponds to an increase in the inductive effect in the transmission line equivalent of the antenna which yields the resonant frequency to shift in lower ranges (Munir et al., 2013; Ng et al., 2018).

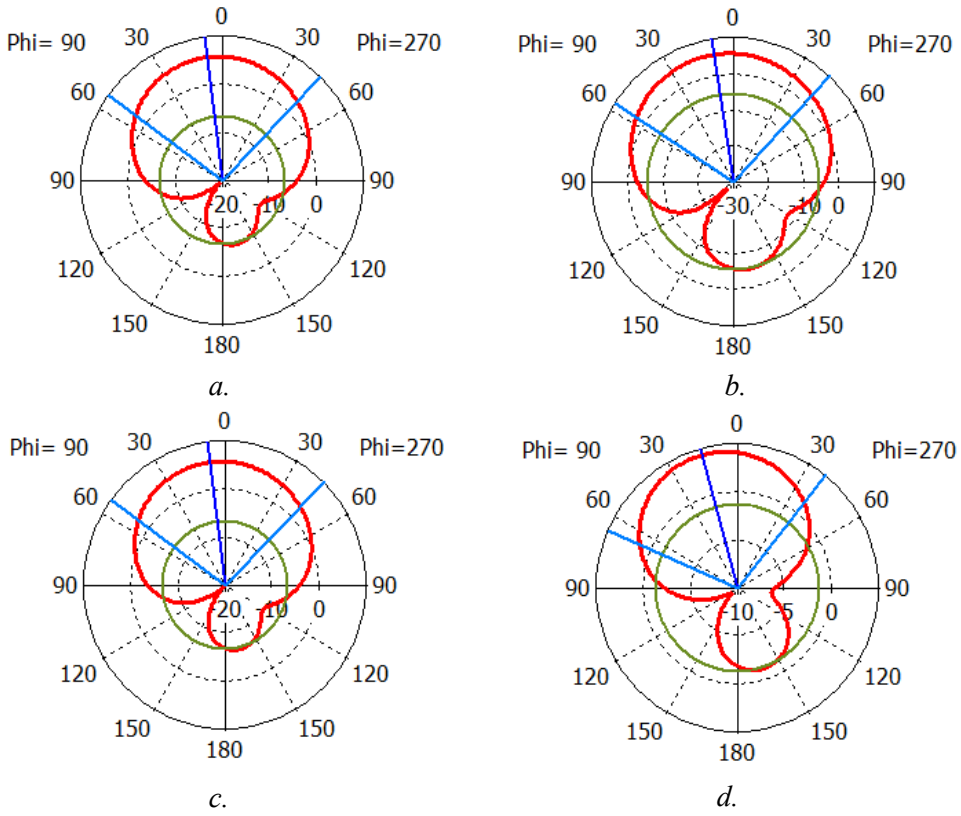

Figure 6:
Far field radiation patterns for proposed antenna models;
a. *Arlon* ***b.*** *Polyamide* ***c.*** *Polyimide* ***d.*** *Silicon*

Figure 6 shows the far-field radiation diagrams for the proposed antennas. The main lobe angles at resonance frequencies for arlon, polyamide, polyimide and silicon materials are 7°, 9°, 7° and 15°, respectively. In addition, the angular width of 3 dB has been observed as 97.4° for arlon, 99.8° for polyamide, 97.8° for polyimide and 104.7° for silicon.

3.2. Performance Analyses of the Slots

Parametric analyzes have been performed about the position of the slots and the edge dimensions for the antennas designed with each material. Thus, the effect of each design parameter on the antenna operating frequencies has been investigated. While performing the analyses, the dimensions with the best results have been chosen as a starting point and the analyzes have been conducted by choosing the appropriate interval steps on these values. For the antenna designed with arlon, Figure 7a shows the changes for the slot edge dimensions of 1 µm, 5 µm and 9 µm. Increasing the edge size has created a negative effect on the return loss levels and has created very little frequency shift. On the other hand, while the position of the slots and their distance from the side and top edges of the antenna changed between 12 µm and 28 µm in 8 µm steps, the operating frequency has not changed, only small fluctuations have been detected in the return loss levels.

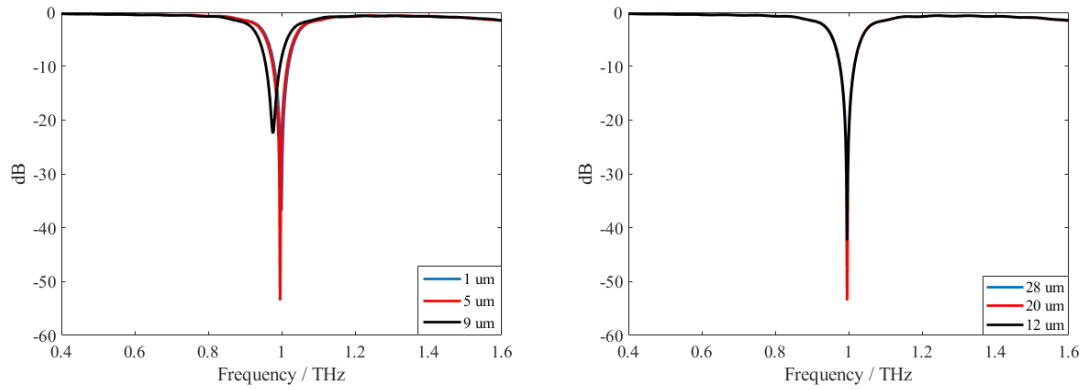

a. *b.*

Figure 7:
Comparison of return loss levels of antennas designed with arlon substrate;
a. *for different slot edges such as a=1 µm;5 µm;9 µm,* ***b.*** *for different positions on the patch, such as b=12 µm;20 µm;28 µm*

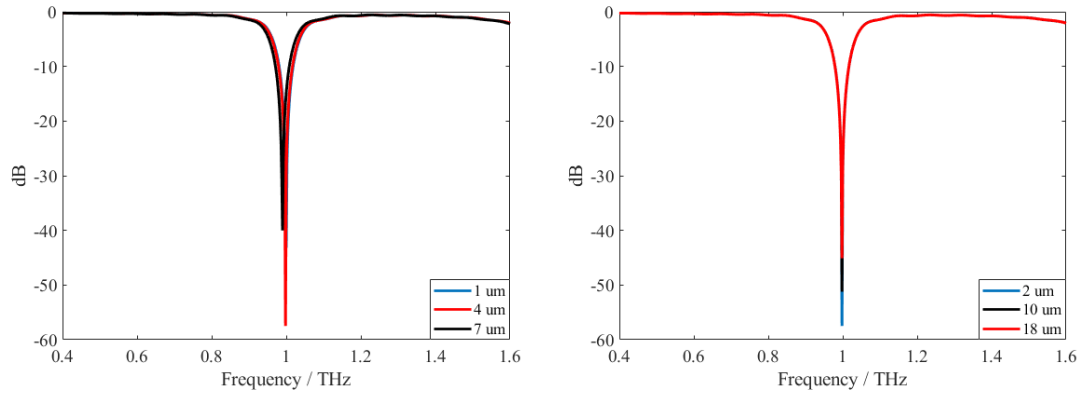

a. *b.*

Figure 8:
Comparison of return loss levels of antennas designed with polyamide substrate;
a. *for different slot edges such as a=1 µm;4 µm;7 µm,* ***b.*** *for different positions on the patch, such as b=2 µm;10 µm;18 µm*

Figures 8a and 8b show the changes of return loss levels for the antenna designed with polyamide material when the slot edge dimensions are 1 µm, 4 µm and 7 µm, respectively, and the distances from the side and top edges of the antenna are 2 µm, 10 µm and 18 µm. Increasing the edge dimensions has yielded little effect on the return loss level and the frequency. Similarly increasing the distances from the edges has little effect on the return loss levels and no effect on operating frequency.

Figures 9a and 9b show the changes of return loss levels for the antenna designed with polyimide substrate when the slot edge dimensions are 6 µm, 11 µm and 16 µm, respectively, and the distances from the side and top edges of the antenna are -5 µm, 0 µm and 5 µm. Negative distance means that the slot protrudes in the outside direction from the edge of the slot and 0 µm means that one corner of the slot is placed on the edge. For polyimide substrate it is clear that the edge

dimensions change effect both on the operating frequency and the return loss level. The increase of the edge dimensions shifts the frequency in lower bands and yields decreased levels for the return loss. However, the change of the location of the slots has almost no effect on the operating frequency and return loss levels.

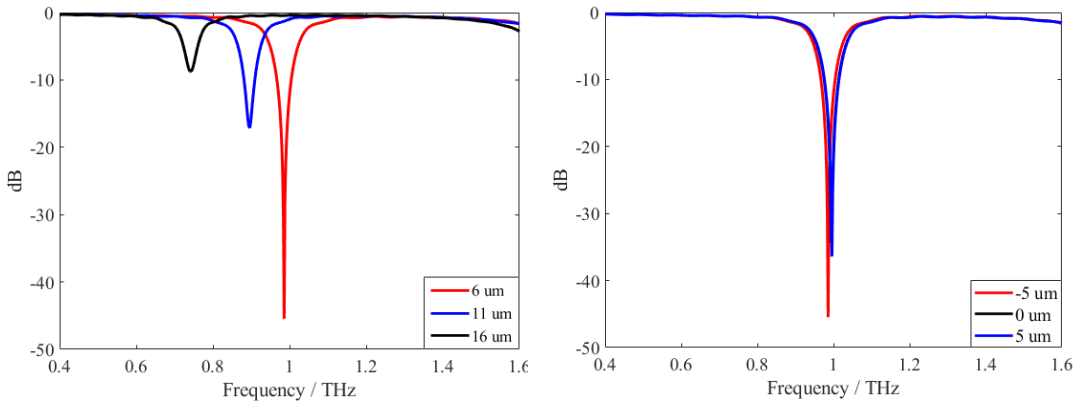

a. *b.*

Figure 9:
Comparison of return loss levels of antennas designed with polyimide substrate; ***a.*** *for different slot edges such as a=6 µm;11 µm;16 µm,* ***b.*** *for different positions on the patch, such as b=-5 µm;0 µm;5 µm*

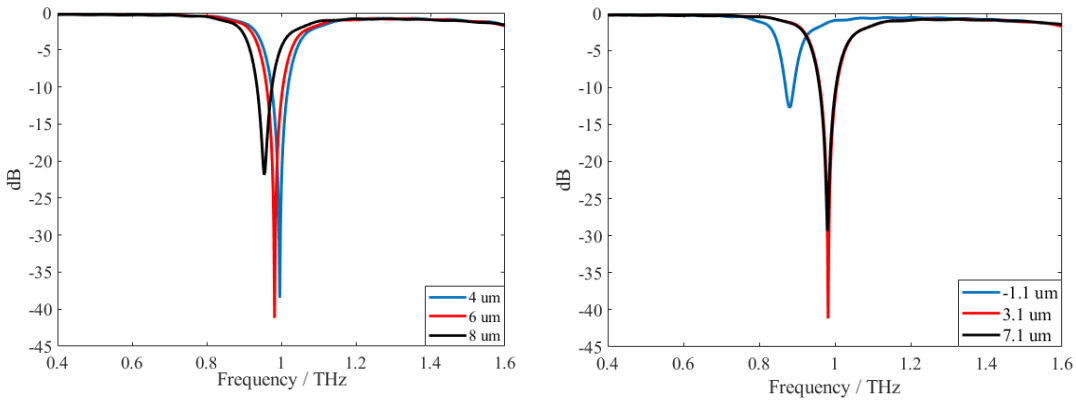

a. *b.*

Figure 10:
Comparison of return loss levels of antennas designed with silicon substrate; ***a.*** *for different slot edges such as a=4 µm; 6 µm;8 µm,* ***b.*** *for different positions on the patch, such as b=1.1 µm;3.1 µm;7.1 µm*

Figures 10a and 10b show the changes of return loss levels for the antenna designed with silicon substrate when the slot edge dimensions are 4 µm, 6 µm and 8 µm, respectively, and the distances from the side and top edges of the antenna are -1.1 µm, 3.1 µm and 7.1 µm. For the return loss level when slot edge dimension increases there occures about 20 dB change after 6 µm but there is no significant change for the frequency. On the other hand the distance variation effects mainly on the frequency when the slot protrudes from the edge. When the plots are examined, the effects

of slot edge sizes have caused significant changes only for the operating frequency in the polyimide substrate antenna and the positions of the slots only changed the return loss and caused a frequency shift only for the silicon substrate. The effect of increasing slot edges on the resonance frequency is seen, especially in Figures 9a and 10a, as a shift to lower ranges for polyimide and silicon substrates due to the increasing value of the inductive effect of the slots (Rahman et al., 2019). Table 5 shows the final values of the design parameters of a and b for the proposed antenna models with different substrate materials.

Table 5. Final design parameter values of slot edges (*a*) and distance amounts from the edges (*b*) for the propsed antenna models with different substrate materials

Arlon		Polyamide	
a	*b*	*a*	*b*
5 µm	20 µm	4 µm	2 µm
Polyimide		Silicon	
a	*b*	*a*	*b*
6 µm	-5 µm	6 µm	3.1 µm

Figure 11 presents the gain plots for the proposed antennas with different substrate materials. It is noted that the gain variation of all antennas tend to increase with the frequency. In addition, the changes of the gain of the antennas with substrates of arlon, polyamide and polyimide are almost the same over the operating frequency range but the antenna with silicon substrate has shown a different gain change variation. This is because thin substrates ($h<<\lambda_0$) with high dielectric constants are less efficient and have greater losses in microstrip antenna design (Ahmed et al., 2006; Roy et al., 2013; Goswami et al., 2012). The maximum gains of the antennas for the resonance frequency are 5.82 dBi, 5.67 dBi, 5.79 dBi and 4.31 dBi for the antennas with the substrates of arlon, polyamide, polyimide and silicon, respectively.

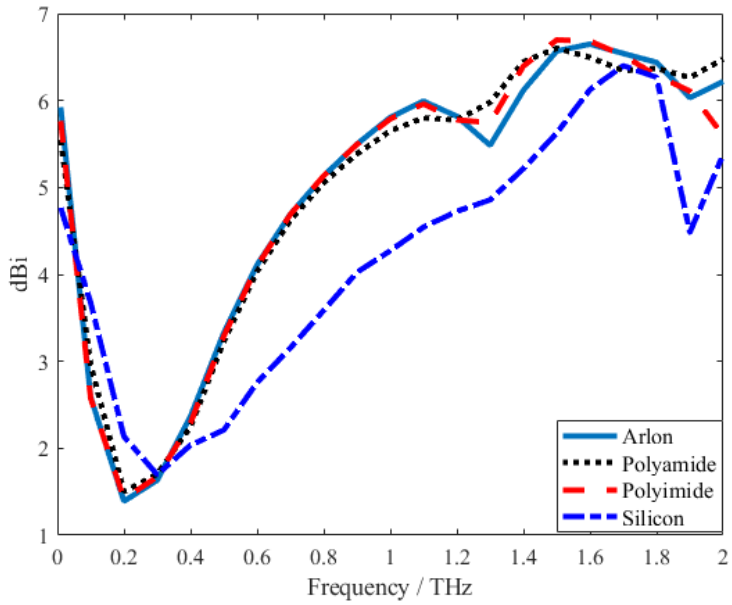

Figure 11:
The gain variation for the proposed antennas

4. CONCLUSION

In this study, a new patch antenna structure is proposed for 6G frequencies. The design is also implemented for different dielectric substrates. There has been different responses in antenna characteristics for each dielectric substrate. In particular, the reductions in return loss level varied widely when comparing the reference antennas and the proposed antennas. Return loss reduction amounts for the antennas with arlon and polyamide substrates have been 38% and 42%, respectively, while the reduction amounts are 28% and 8% for the antennas with polyimide and silicon substrates, respectively. In the far field radiation characteristics, the main lobe angle at the resonance frequency is between 7° and 9° for arlon, polyamide and polyimide, while this value is 14° for the silicon substrate. For the bandwidth variation, arlon has created the least change, while maximum increase is with the polyimide substrate. With these results, the proposed design can be used as a new structure for 6G communication systems, and a comparison between materials is provided by realizing the same design on different dielectric substrates. In addition, this study will provide an idea for the investigation of material effects in 6G multi-antenna structures.

CONFLICT OF INTERESTS

The author declares that he has no actual, potential, or perceived conflict of interest for this article.

AUTHOR CONTRIBUTION

Barış Gürcan Hakanoğlu confirms sole responsibility for preparing the manuscript, including designing and performing simulations, data collection, analysis, interpretation of results, and writing and editing the manuscript.

REFERENCES

1. Giordani, M., Polese, M., Mezzavilla, M., Rangan, S., Zorzi, M. (2020) Toward 6G Networks: Use Cases and Technologies. *IEEE Communications Magazine*, 58(3), 55-61. doi: 10.1109/MCOM.001.1900411

2. Yang, P., Xiao, Y., Xiao, M., Li, S. (2019) 6G Wireless Communications: Vision and Potential Techniques. *IEEE Network*, 33(4), 70-75. doi: 10.1109/MNET.2019.1800418

3. You, X., Wang, CX., Huang, J. et al. (2021) Towards 6G wireless communication networks: vision, enabling technologies, and new paradigm shifts. *Sci. China Inf. Sci. 64*, 110301. https://doi.org/10.1007/s11432-020-2955-6

4. Chowdhury, M. Z., Shahjalal, M., Ahmed, S., Jang, Y. M. (2020) 6G Wireless Communication Systems: Applications, Requirements, Technologies, Challenges, and Research Directions. *IEEE Open Journal of the Communications Society*, 1, 957-975. doi:10.48550/arXiv.1909.11315

5. Alsharif, M. H., Kelechi, A. H., Albreem, M. A., Chaudhry, S. A., Zia, M. S., Kim, S. (2020) Sixth generation (6G) wireless networks: Vision, research activities, challenges and potential solutions. *Symmetry*, 12(4), 676. https://doi.org/10.3390/sym12040676

6. Strinati, E. C., Peeters, M., Neve, C. R., Gomony, M. D., Cathelin, A., Boldi, M. R., Belot, D. (2022) The Hardware Foundation of 6G: The NEW-6G Approach. *IEEE Joint European Conference on Networks and Communications & 6G Summit (EuCNC/6G Summit)*, pp. 423-428. doi: 10.1109/EuCNC/6GSummit54941.2022.9815700

7. Foysal, M. F., Mahmud, S., Baki, A. K. M. (2021) A novel high gain array antenna design for autonomous vehicles of 6g wireless systems. *IEEE International Conference on Green*

Energy, Computing and Sustainable Technology (GECOST), 1-5. doi: 10.1109/GECOST52368.2021.9538677

8. Ilahi, F., Dutta, S., Hasan, M. M., Rumpa, S. A., Baki, A. K. M. (2021) Development of a Novel UWB Antenna for 6G-IoT Based Smart Grid Device Monitoring System. *IEEE International Conference on Green Energy*, Computing and Sustainable Technology (GECOST), 1-5. doi: 10.1109/GECOST52368.2021.9538785

9. Singhal, S. (2019) Ultrawideband elliptical microstrip antenna for terahertz applications. *Microwave and Optical Technology Letters*, 61(10), 2366-2373. https://doi.org/10.1002/mop.31910

10. Chung, M. A., Chuang, B. R. (2021) Design a Broadband U-Shaped Microstrip Patch Antenna on Silicon-Based Technology for 6G Terahertz (THz) Future Cellular Communication Applications. *10th International Conference on Internet of Everything, Microwave Engineering, Communication and Networks (IEMECON)*, 1-5. doi: 10.1109/IEMECON53809.2021.9689167

11. Bala, R., Marwaha, A. (2016) Characterization of graphene for performance enhancement of patch antenna in THz region. *Optik*, 127(4), 2089-2093. https://doi.org/10.1016/j.ijleo.2015.11.029

12. Azizi, M. K., Ksiksi, M. A., Ajlani, H., Gharsallah, A. (2017) Terahertz graphene-based reconfigurable patch antenna. *Progress In Electromagnetics Research Letters*, 71, 69-76. http://dx.doi.org/10.2528/PIERL17081402

13. Anand, S., Kumar, D. S., Wu, R. J., Chavali, M. (2014) Graphene nanoribbon based terahertz antenna on polyimide substrate. *Optik*, 125(19), 5546-5549. https://doi.org/10.1016/j.ijleo.2014.06.085

14. Dashti, M., Carey, J. D. (2018) Graphene microstrip patch ultrawide band antennas for THz communications. *Advanced Functional Materials*, 28(11), 1705925. https://doi.org/10.1002/adfm.201705925

15. Khan, M. A. K., Shaem, T. A., Alim, M. A. (2020) Graphene patch antennas with different substrate shapes and materials. *Optik*, 202, 163700. https://doi.org/10.1016/j.ijleo.2019.163700

16. Efazat, S. S., Basiri, R., & Makki, S. V. A. D. (2019) The gain enhancement of a graphene loaded reconfigurable antenna with non-uniform metasurface in terahertz band. *Optik*, 183, 1179-1190. https://doi.org/10.1016/j.ijleo.2019.02.034

17. Khan, M. A. K., Shaem, T. A., Alim, M. A. (2019) Analysis of graphene based miniaturized terahertz patch antennas for single band and dual band operation. *Optik*, 194, 163012. https://doi.org/10.1016/j.ijleo.2019.163012

18. Computer Simulation Technology (CST) Microwave Studio, Ver. 2016, Framingham, MA, USA, 2016.

19. Balanis, A. (2005) *Antenna Theory*, John Wiley&Sons, Hoboken, New Jersey.

20. Stutzmann, W. L., Thiele, G. A. (1998) *Antenna Theory and Design*, John Wiley&Sons, Hoboken, New Jersey.

21. Munir, A., Petrus, G., & Nusantara, H. (2013). Multiple slots technique for bandwidth enhancement of microstrip rectangular patch antenna. *IEEE International Conference on QiR*, 150-154.

22. Ng, W. H., Lim, E. H., Bong, F. L., & Chung, B. K. (2018). Folded patch antenna with tunable inductive slots and stubs for UHF tag design. *IEEE Transactions on Antennas and Propagation*, *66*(6), 2799-2806.

23. Rahman, M. M., Islam, M. S., Wong, H. Y., Alam, T., & Islam, M. T. (2019). Performance analysis of a defected ground-structured antenna loaded with stub-slot for 5G communication. *Sensors*, *19*(11), 2634.

24. Ahmed, A. K. and S.M. Juma, S. M. (2006). Cavity Model Analysis of Rectangular Microstrip Antenna. *IEEE Trans.*.

25. Roy, A. A., Môm, J. M., Kureve D. T. (2013). Effect of dielectric constant on the design of rectangular microstrip antenna. *IEEE International Conference on Emerging & Sustainable Technologies for Power & ICT in a Developing Society (NIGERCON)*, 111-115.
26. Goswami, K. (2012). Study of Microstrip Slotted Antenna for Bandwidth Enhancement. *Global Journal of Researches in Engineering Electrical and Electronics Engineering*, 12(9).